

by *in situ* X-ray observations based on the same pressure scale in the previous study^{13,14}. The overpressure was calculated using these boundaries. We observed the pressure to drop during the transformation by 1–2 GPa, but this would not affect the transformation rate significantly because the overpressure is very large in the present study. This has been confirmed in the post-spinel transformation⁷.

One starting material was a powdered mixture of natural pyrope and gold. In experiments using the natural pyrope, the sample was annealed at 20 GPa and 1,523 K for 2 h before the transformation to achieve equilibrium microstructures, resulting in equigranular polycrystalline pyrope of $12 \pm 2 \mu\text{m}$ in diameter. Another starting material was a sintered mixture of pure pyrope and gold, which was synthesized at 20 GPa and 1,773 K using the pyrope glass. The sintered pure pyrope was not annealed before the transformation because equilibrium microstructures in the sintered sample are almost maintained during the cold compression stage⁷. The grain size of pure pyrope was $3.2 \pm 0.5 \mu\text{m}$. After the pressure reached the desired value, the sample was heated at a rate of 500 K min^{-1} . When the temperature reached the desired value, it was kept constant and X-ray diffraction patterns of the sample were taken every 10–300 s by the energy dispersive method using a Ge solid-state detector. The transformed volume fraction was estimated on the basis of the integrated intensity of diffraction lines 400, 642 in pyrope relative to the intensity before the transformation⁷. We observed uniform changes of the diffraction peaks during the transformation, which is diagnostic of the absence of a preferred orientation.

Received 29 July; accepted 25 October 2002; doi:10.1038/nature01281.

- Hirose, K., Fei, Y., Ma, Y. & Mao, H. K. The fate of subducted basaltic crust in the Earth's lower mantle. *Nature* **397**, 53–56 (1999).
- Akaogi, M. & Ito, E. Calorimetric study on majorite-perovskite transition in the system $\text{Mg}_3\text{Si}_2\text{O}_{12}$ - $\text{Mg}_3\text{Al}_2\text{Si}_2\text{O}_{12}$: transition boundaries with positive pressure-temperature slopes. *Phys. Earth Planet. Inter.* **114**, 129–140 (1999).
- Irifune, T. & Ringwood, A. E. Phase transformations in subducted oceanic crust and buoyancy relationships at depths of 600–800 km in the mantle. *Earth Planet. Sci. Lett.* **117**, 101–110 (1993).
- Ringwood, A. E. Role of the transition zone and 660 km discontinuity in mantle dynamics. *Phys. Earth Planet. Inter.* **86**, 5–24 (1994).
- Kesson, S. E., Fitz Gerald, J. D. & Shelley, J. M. G. Mineral chemistry and density of subducted basaltic crust at lower-mantle pressures. *Nature* **372**, 767–769 (1994).
- Faust, J. & Knittle, E. The stability and equation of state of majoritic garnet synthesized from natural basalt at mantle conditions. *Geophys. Res. Lett.* **23**, 3377–3380 (1996).
- Kubo, T. *et al.* Mechanisms and kinetics of the post-spinel transformation in Mg_2SiO_4 . *Phys. Earth Planet. Inter.* **129**, 153–171 (2002).
- Kawai, N. & Endo, S. The generation of ultrahigh hydrostatic pressures by a split sphere apparatus. *Rev. Sci. Instrum.* **41**, 1178–1181 (1970).
- Ohtani, E. *et al.* High pressure generation by a multiple anvil system with sintered diamond anvils. *Rev. Sci. Instrum.* **60**, 922–925 (1989).
- Kondo, T. *et al.* Ultrahigh-pressure and high-temperature generation by use of the MA-8 system with sintered-diamond anvils. *High Temp. High Press.* **25**, 105–112 (1993).
- Kato, T., Ohtani, E., Kamaya, N., Shimomura, O. & Kikegawa, T. *High Pressure Research in Mineral Physics: Application to Earth and Planetary Sciences* (eds Syono, Y. & Manghni, M. H.) 33–36 (Geophysical Monograph 67, American Geophysical Union, Washington DC, 1992).
- Kato, T. *et al.* *In situ* X ray observation of high-pressure phase transitions of MgSiO_3 and thermal expansion of MgSiO_3 perovskite at 25 GPa by double-stage multianvil system. *J. Geophys. Res.* **100**, 20475–20481 (1995).
- Hirose, K., Fei, Y., Ono, S., Yagi, T. & Yagi, T. *In situ* measurements of the phase transition boundary in $\text{Mg}_3\text{Al}_2\text{Si}_2\text{O}_{12}$: implications for the nature of the seismic discontinuities in the Earth's mantle. *Earth Planet. Sci. Lett.* **184**, 567–573 (2001).
- Oguri, K. *et al.* Post-garnet transition in a natural pyrope: a multi-anvil study based on *in situ* X-ray diffraction and transmission electron microscopy. *Phys. Earth Planet. Inter.* **122**, 175–186 (2000).
- Miyajima, N., Fujino, K., Funamori, N., Kondo, T. & Yagi, T. Garnet-perovskite transformation under conditions of the Earth's lower mantle: an analytical transmission electron microscopy. *Phys. Earth Planet. Inter.* **116**, 117–131 (1999).
- Poirier, J. P., Peyronneau, J., Madon, M., Guyot, F. & Revcolevschi, A. Eutectoid phase transformation of olivine and spinel into perovskite and rock salt structures. *Nature* **321**, 603–605 (1986).
- Kubo, T. *et al.* Formation of metastable assemblages and mechanisms of the grain-size reduction in the postspinel transformation of Mg_2SiO_4 . *Geophys. Res. Lett.* **27**, 807–810 (2000).
- Cahn, J. W. The kinetics of grain boundary nucleated reactions. *Acta Metall.* **4**, 449–459 (1956).
- Kirby, S. H., Stein, S., Okal, E. A. & Rubie, D. C. Metastable mantle phase transformations and deep earthquakes in subducting oceanic lithosphere. *Rev. Geophys.* **34**, 261–306 (1996).
- Riedel, M. R. & Karato, S. Grain-size evolution in subducted oceanic lithosphere associated with the olivine-spinel transformation and its effects on rheology. *Earth Planet. Sci. Lett.* **148**, 27–43 (1997).
- Ono, S., Ito, E. & Katsura, T. Mineralogy of subducted basaltic crust (MORB) from 25 to 37 GPa, and chemical heterogeneity of the lower mantle. *Earth Planet. Sci. Lett.* **190**, 57–63 (2001).
- Karato, S. On the separation of crustal component from subducted oceanic lithosphere near the 660 km discontinuity. *Phys. Earth Planet. Inter.* **99**, 103–111 (1997).
- Kawakatsu, H. & Niu, F. Seismic evidence for a 920-km discontinuity in the mantle. *Nature* **371**, 301–305 (1994).
- Niu, F. & Kawakatsu, H. Depth variation of the mid-mantle seismic discontinuity. *Geophys. Res. Lett.* **24**, 429–432 (1997).
- Pawley, A. R., McMillan, P. F. & Holloway, J. R. Hydrogen in stishovite, with implications for mantle water content. *Science* **261**, 1024–1026 (1993).
- Irifune, T. *et al.* *Properties of Earth and Planetary Materials at High Pressure and Temperature* (eds Manghni, M. H. & Yagi, T.) 1–8 (Geophysical Monograph 101, American Geophysical Union, Washington DC, 1998).
- Anderson, O. L., Issak, D. G. & Yamamoto, S. Anharmonicity and the equation state for gold. *J. Appl. Phys.* **6**, 1534–1543 (1989).
- Dziewonski, A. M. & Anderson, D. L. Preliminary reference Earth model. *Phys. Earth Planet. Inter.* **25**, 297–356 (1981).

Acknowledgements We thank D. H. Green and B. Hiberson for discussions and information on the larger ADC anvil, and K. Fujino for providing natural pyrope crystal and comments. This work was partially supported by the Grant-in-Aid for Scientific Research from the Ministry of Education, Culture, Sports, Science and Technology, Japan.

Competing interests statement The authors declare that they have no competing financial interests.

Correspondence and requests for materials should be addressed to T. Kubo (e-mail: tkubo@mail.cc.tohoku.ac.jp).

SAR11 clade dominates ocean surface bacterioplankton communities

Robert M. Morris*, Michael S. Rappé*, Stephanie A. Connon*, Kevin L. Vergin*, William A. Siebold*, Craig A. Carlson† & Stephen J. Giovannoni*

* Department of Microbiology, Oregon State University, Corvallis, Oregon 97331, USA

† Department of Ecology, Evolution and Marine Biology, University of California, Santa Barbara, California 93106-9610, USA

The most abundant class of bacterial ribosomal RNA genes detected in seawater DNA by gene cloning belongs to SAR11—an α -proteobacterial clade¹. Other than indications of their prevalence in seawater, little is known about these organisms. Here we report quantitative measurements of the cellular abundance of the SAR11 clade in northwestern Sargasso Sea waters to 3,000 m and in Oregon coastal surface waters. On average, the SAR11 clade accounts for a third of the cells present in surface waters and nearly a fifth of the cells present in the mesopelagic zone. In some regions, members of the SAR11 clade represent as much as 50% of the total surface microbial community and 25% of the subeuphotic microbial community. By extrapolation, we estimate that globally there are 2.4×10^{28} SAR11 cells in the oceans, half of which are located in the euphotic zone. Although the biogeochemical role of the SAR11 clade remains uncertain, these data support the conclusion that this microbial group is among the most successful organisms on Earth.

Comprehensive information is available about the overall abundance of marine bacterioplankton, which dominate living biomass and have a chief ecological role in marine food webs^{2–5}. With the exception of marine Archaea^{6,7}, however, there is very little quan-

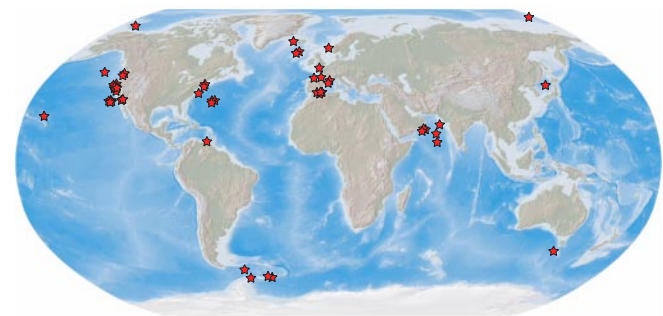


Figure 1 Distribution of the SAR11 clade in the world's oceans. Red marks indicate locations where SAR11 ribosomal RNA genes have been detected using molecular techniques. Although 52 individual samples are represented, many studies along the US Pacific coast and in the North Atlantic have been conducted at the same sample locations and are therefore represented by a single red mark.

titative information about the cellular abundance of specific phylogenetic groups of marine microorganisms. Most knowledge about bacterioplankton diversity comes from 16S ribosomal RNA gene (ribosomal DNA) cloning studies, which have identified several groups of marine bacteria that are thought to be abundant in seawater¹. Although members of the SAR11 clade have no ascribed physiology, they consistently dominate 16S rDNA clone libraries. They have been present in over 50 studies of marine bacterioplankton microbial diversity from sites around the globe (Fig. 1) and account for 25% of all the genes recovered in these studies. Although gene clone library data strongly support the importance of the SAR11 clade in the oceans, these data are open to considerable interpretation, owing to the uncertainties associated with the specificity of polymerase chain reaction (PCR) amplification primers, ribosomal RNA gene copy number and other factors⁸.

In August 2001, seawater samples were collected along a meridional transect in the northwestern Sargasso Sea. Additional samples collected from the Bermuda Atlantic Time-series Study (BATS) site in February and March 2001 were also processed for abundance during winter and spring periods. Surface samples (10 m depth) from the Oregon coast were collected along the Newport Hydroline at station NH5 (44° 39.1' N, 124° 10.6' W) in September 2001 and February 2002, where average nutrient content and productivity are markedly higher than in the western Sargasso Sea. Four Cy3-labelled oligonucleotide probes targeting SAR11 clade 16S rRNA and five Cy3-labelled oligonucleotide probes targeting bacterial 16S rRNA were used in separate hybridization reactions. Digital processing of raw images was used to restrict counting to cells showing fluorescence from both the Cy3 probe and the nucleic acid dye 4',6-diamidino-2-phenylindole dihydrochloride (DAPI)⁹. With this approach, there was very little ambiguity in determining cell counts.

Unlike gene cloning, fluorescence *in situ* hybridization (FISH) is an accurate method for determining the exact abundance of cells in natural samples^{10–12}, provided that the probes circumscribe their phylogenetic target and the fluorescence signals from cells are high enough for consistent scoring. Because some microbial cells, such as small, slow-growing bacterioplankton, are difficult to detect by this method, various strategies have been used to increase signal intensity and counting accuracy. Some of these studies have focused primarily on probe design^{13,14}, whereas others have explored strategies to amplify the fluorescent signal per cell^{15–17}. Our strategy was to use several probes that target different regions of the 16S rRNA to produce an additive effect on signal intensity, coupled with a sensitive cooled CCD (charge-coupled device) camera for detecting

low levels of fluorescence. Our measurements of bacterial abundances were equivalent to those obtained with polynucleotide probes (poly-FISH) in coastal North Sea and Monterey Bay Californian samples¹⁸. The high quantum efficiency of cooled CCD cameras makes it theoretically possible to detect single probe molecules; thus, in hybridization experiments such as these the real limitations are the signal-to-noise ratio achieved and the specificity of the probes.

Analyses of hybridization images showed that cells hybridizing to the SAR11 probes were abundant curved rods of less than 1 μm (Fig. 2). These accounted for 35% ($n = 24$) and 18% ($n = 7$) of total microbial cell abundance in the euphotic and mesopelagic zones, respectively. There was no discernible difference in the morphology of SAR11 cells from the different oceans, or from different depths in the Atlantic. The biovolume of SAR11 cells relative to the average for the marine bacterioplankton community was determined from the ratio of the average areas of SAR11 cell images ($n = 175$) and bacterial cell images ($n = 257$) by assuming that the cells were prolate spheroids¹⁹. The biovolume of SAR11 cells was inferred to be roughly half of the average biovolume for cells in the bacterioplankton community.

Depth profiles showed that members of the SAR11 clade were numerically abundant throughout the water column in the western Atlantic, averaging 2.0×10^8 cells l^{-1} ($n = 24$) within and 0.2×10^8 cells l^{-1} ($n = 7$) below the euphotic zone (>150 m; Fig. 3). Cell counts determined with DAPI averaged 5.7×10^8 cells l^{-1} ($n = 72$) within and 1.2×10^8 cells l^{-1} ($n = 21$) below the euphotic zone. To ensure that cells were not being removed in the hybridization process, direct cell counts determined from hybridization preparations were compared with independent preparations that used standard DAPI staining procedures for counting cells²⁰. Agreement between the values was 99.6% in pair-wise comparisons, showing that most cells remained on the filters throughout the hybridization procedure.

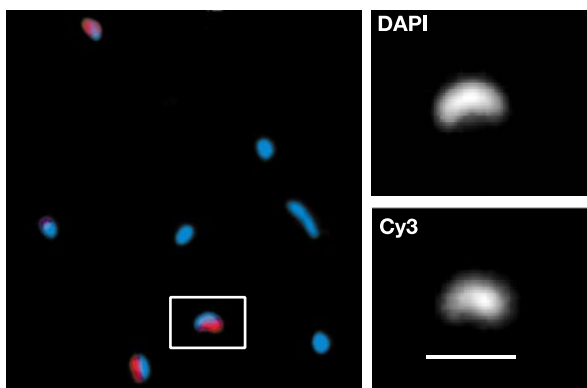


Figure 2 SAR11 fluorescence *in situ* hybridization image composite. Dual image overlay of DNA-containing cells stained with DAPI (blue) and the Cy3 probe (red). Cells emitting a signal for both DAPI and the Cy3 probe are both blue and red, and cells that did not hybridize to the set of SAR11 probes are blue. The identical fields of view in the DAPI- and Cy3-stained images show the characteristic size and curved rod morphology of a magnified SAR11 cell (white box). Scale bar, 1 μm.

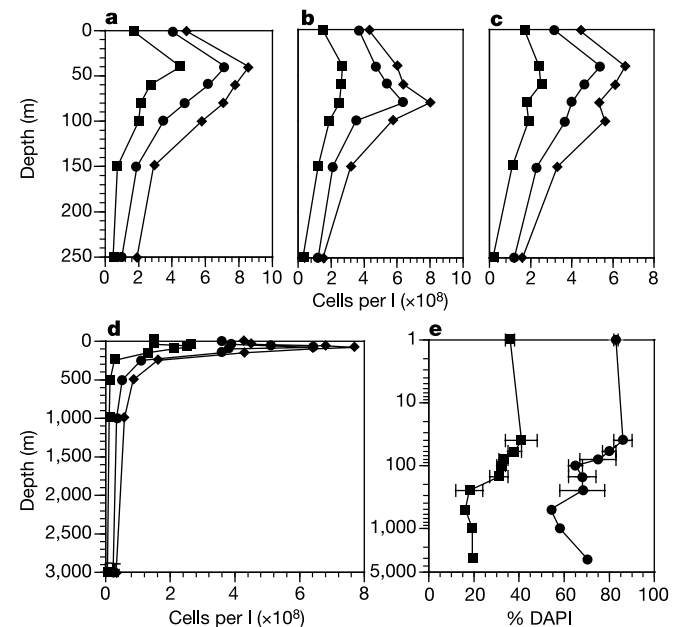


Figure 3 SAR11 probe counts, bacterial probe counts and direct cell counts (DAPI-staining particles) in the northwestern Sargasso Sea. **a–d**, SAR11 clade (squares), Bacteria (circles) and DAPI (diamonds) counts at 32° N, 64° W (CDOM-01; BATS site; **a**), 30° N, 64° W (CDOM-03; **b**), 28° N, 64° W (CDOM-05; **c**) and 26° N, 64° W (CDOM-07; **d**). **e**, A transect composite shows the mean abundance values by depth for SAR11 clade and bacterial cell counts as percentages of direct cell counts (DAPI staining particles); $n = 4$, except for depths below 250 m, where $n = 1$. Standard deviations are given for depths of 1–250 m. One sample point was obtained for depths below 250 m at 26° N, 64° W (CDOM-07).

Probe counts were compared with total DAPI cell counts from the same samples to determine the relative abundances of the SAR11 clade and domain Bacteria. Results from a mean composite of all Atlantic transect profiles indicated that SAR11 accounted for 31–41% of the total DAPI cell counts within the euphotic zone, and 16–19% between 250 and 3,000 m (Fig. 3). The relative abundance of SAR11 exceeded 40% in several profiles and accounted for 51% of the microbial community in the 40-m sample from the BATS site (CDOM-01). Data from samples collected at BATS in February and March 2001 showed similarly high cellular abundances of SAR11 cells in winter months (data not shown). On average, SAR11 cells accounted for 35% ($n = 8$) of the total DAPI cell counts in surface waters to 200 m, and 16% ($n = 5$) at depths from 250 m to 3,600 m. The relative abundance of the SAR11 clade in Oregon coastal surface samples was 17% in September 2001 and 38% in February 2002.

Transect averages showing the relative contribution of cells counted with the bacterial probe suite to total DAPI cell counts ranged from 65 to 86% in the upper ocean surface, reaching maximum values in the surface 40 m (Fig. 3). These values were corrected by subtracting the autofluorescent cell counts obtained from duplicate slides hybridized to the negative control probe. This procedure may result in an underestimate of the total number of cells detected with the bacterial probes, because autofluorescent cells, including cyanobacteria, were excluded. The bacterial contribution to total DAPI cell counts declined to 54% between 250 and 3,000 m. Although bacterial cell counts may be underestimated because some cells fail to produce a probe signal that is sufficient to raise the detection level above background, these observations are consistent with previous findings of a significant archaeal contribution to picoplankton abundance in the mesopelagic⁶.

Hybridization of radioactive probes to bulk RNA extracted from the same samples and from monthly time-series samples collected at the BATS site between September 1997 and August 2000 showed a similar trend in the vertical distribution of SAR11 clade rRNA (Fig. 4). In transect samples taken in August 2001, the percentage of bacterial 16S rRNA contributed by the SAR11 clade varied from 18% ($n = 3$) in the euphotic zone to 3% ($n = 4$) in the aphotic zone (Fig. 4b). Monthly time-series data produced similar values and showed an annual trend in SAR11 clade 16S rRNA abundance (Fig. 4a). Maximal values occurred in the summer, when SAR11 clade 16S rRNA accounted for as much as 32%, 26% and 28% of all bacterial 16S rRNA present in surface waters at the BATS site (June–July 1998, August 1999 and August 2000, respectively). Note that the relatively low temporal variability of total DAPI counts

(Fig. 4c), despite a temporally dynamic SAR11 population, suggests the possibility that other prokaryotic populations are changing as well. SAR11 SSU rRNA percentages are less than the measured percentages of SAR11 cells for the same depth strata, probably because SAR11 cells are unusually small and ribosome content is correlated with cell volume²¹. SAR11 cells have been cultured in our laboratory, and SAR11 biovolumes have been estimated to be about $0.01 \mu\text{m}^3$ from electron micrograph data²². These results and the image data discussed above indicate that the SAR11 contribution to marine biomass is less than their absolute numbers would suggest.

A previous study that used a single oligonucleotide probe to count SAR11 cells in coastal water samples reported that SAR11 abundance was low (<1% of total marine microbial abundance)²³. That result may reflect a real variation in SAR11 abundance; alternatively, single oligonucleotide probes might undercount their target if signals from some cells fall below the background fluorescence of the *in situ* hybridization preparation, which is particularly likely to occur when the target cells are unusually small¹⁸.

Data showing a global distribution of SAR11 (Fig. 1), and the consistent cell counts that we obtained from highly disparate sites, suggest that global extrapolation from our data is justified. Using our mean percentages for surface and mesopelagic samples and previous reported values²⁴, which estimated that globally there are 3.6×10^{28} prokaryotic cells in the upper 200 m of the ocean surface and 6.5×10^{28} prokaryotic cells below 200 m, we calculate that the global abundance of SAR11 in the oceans is 2.4×10^{28} cells. Previous studies⁶ have calculated the abundance of the pelagic crenarchaeota clade to be of the same order as our estimates for the SAR11 clade, 1.3×10^{28} archaeal cells, and have calculated bacterial cell numbers of 3.1×10^{28} cells. On the basis of previous calculations^{6,24} of total global ocean prokaryotic cell abundance, we estimate that SAR11 contributes 24–55% of oceanic prokaryotic cells. Using estimates of global ocean prokaryotic abundance²⁴ and the relative cell sizes measured by microscopic imaging, we calculate that SAR11 cells account for 18% of the total bacterial biomass in surface waters (upper 200 m) and for 9% in deeper waters (200–3,000 m), assuming that the average SAR11 cell contains roughly half as much carbon per cell as the average for marine bacteria. Overall, we estimate that SAR11 contributes about 12% of total marine prokaryotic biomass. Although approximations, these numbers highlight the magnitude of global SAR11 clade populations.

Dividing SAR11 cells were observed in Sargasso Sea samples from all depths, suggesting that members of this clade are actively

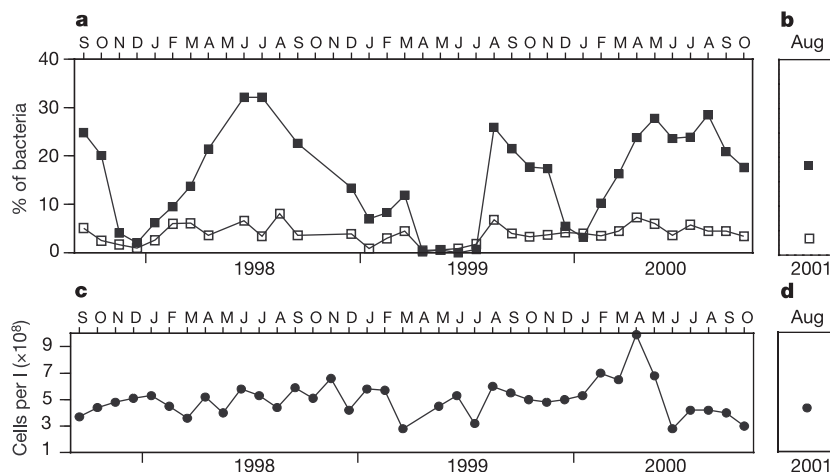


Figure 4 Percentages of SAR11 clade 16S rRNA at surface depths and depths ≥ 200 m. **a**, Monthly time-series samples from the BATS site for surface (filled squares) and 200-m depths (open squares) over a 3-yr period. **b**, August 2001 transect averages for surface ($n = 3$) and ≥ 200 m ($n = 4$) depths from CDOM-03

(1 m), CDOM-05 (1, 250 m) and CDOM-07 (1, 250, 1,000 and 3,000 m). **c**, Corresponding total prokaryotic abundance (filled circles) in the surface 5 m for the BATS time series data, estimated by direct counting with DAPI. **d**, Average prokaryotic abundance from 1 m (CDOM-01, CDOM-03, CDOM-05 and CDOM-07).

replicating throughout the water column. Although exponentially growing cultures can be readily distinguished from stationary-phase cultures by the presence of dividing cells in the former, we were unable to make quantitative estimates of the *in situ* growth rates of SAR11 cells by measuring the frequency of dividing cells. The noise in image analysis parameters associated with cell shape is inherently high when viewing cells that have a size close to the limit of resolution of light microscopy.

Although the SAR11 clade probe suite used in this study did not distinguish between different SAR11 lineages, previous work has shown that different phylogenetic groups within the SAR11 clade are found in different regions of the water column²⁵. It is unknown whether this phylogenetic differentiation is associated with specialization in the use of nutrient resources. The numbers of SAR11 cells indicated by this study suggest that these organisms are efficient competitors for resources that are available throughout the water column. Our results do not rule out the possibility that other microorganisms may grow more rapidly than SAR11 but may be less abundant because grazing, viral predation or other sources of mortality result in a high rate of cell removal. Genome sequencing of SAR11 is now in progress, and future research will undoubtedly seek to identify specifically the physiological activities of these cells and their role in the oceanic carbon cycle. □

Methods

Sample collection

We collected water from four transect stations in the northwestern Sargasso Sea. Samples from ten depths between 1 and 3,000 m were collected in Niskin bottles on a 24-place conductivity-temperature-density device rosette and transferred to primary collection bottles. Subsample volumes of 10–40 ml were immediately fixed in filtered paraformaldehyde at a final concentration of 3% and stored at 4 °C for 6–8 h. Fixed samples were filtered onto white 0.2-µm Osmonics polycarbonate filters, placed immediately in slide boxes containing silicon desiccant and stored at –20 °C.

Probe analysis

We analysed 261 SAR11 and 12,300 total 16S rRNA sequences using the ARB sequence analysis package²⁶ to determine probe specificity and accuracy. A total of 149 SAR11 sequences contained sequence spanning at least one target site, and 133 contained an exact match to at least one probe sequence. A minimum of three of the four probes matched exactly all rRNA genes with sequence spanning all target sites (*n* = 27), and most of these sequences (66%) matched all four probes identically. None of the probes used in the SAR11 probe suite matched sequences outside the SAR11 clade. The oligonucleotide probes used to enumerate members of the SAR11 clade were as follows: SAR11-152R (5'-ATTAG CACAAGTTTCCYCGTGT-3'), SAR11-441R (5'-TACAGTCATTTCCTCCCCGAC-3'), SAR11-542R (5'-TCCGAAGTACGCTAGGTC-3'), and SAR11-732R (5'-GTCAGTAATG ATCCAGAAAGYTG-3'). The oligonucleotide probes used to enumerate Bacteria were as follows: EUB-27R (5'-CTGAGCCAKGATCRAACTCT-3'), EUB-338Rpl (5'-GCWGCC WCCCGTAGGWT-3'), EUB-700R (5'-CTAHGCAATTCACYGCTACAC-3'), EUB-700Ral (5'-CTACGAATTCACCTCTACAC-3') and EUB-1522R (5'-AAGGAGGTGAT CCANCCVCA-3'). The negative control oligonucleotide was 338F (5'-TGAGGATGCC CCGCTCG-3').

FISH

Hybridization reactions were carried out essentially as described¹² with the following modifications. Reactions were done on one-quarter membrane sections at 37 °C for 16 h in hybridization buffer (900 mM NaCl, 20 mM Tris (pH 7.4), 0.01% (w/v) SDS, 15% formamide) and either SAR11 or Bacteria-specific Cy3-labelled oligonucleotide probes. Individual probes in each set of probes were each used at a final concentration of 2 ng µl⁻¹. We also used a Cy3-labelled nonsense oligonucleotide (338F) as a negative control at a final concentration of 8 ng µl⁻¹. Optimal hybridization stringency was achieved by washing the membranes in hybridization wash (150 mM NaCl, 20 mM Tris (pH 7.4), 6 mM EDTA and 0.01% SDS) for two 10-min intervals at experimentally determined temperatures of dissociation (*T_d*) specific for the individual sets of probes (SAR11, 55 °C; Bacteria, 50 °C; 338F, 50 °C). Nucleic acid staining was achieved by transferring the membrane to hybridization wash containing 5 µg ml⁻¹ DAPI for 10 min at 4 °C. DAPI was rinsed off for 2 min in a final hybridization wash at 4 °C. All reagents were filtered through 0.2-µm membranes.

Fluorescent microscopy

After mounting the filters in Citifluor (Ted Pella), Cy3-positive and DAPI-positive cells were counted for each field of view using a Leica DMRB epifluorescence microscope equipped with a Hamamatsu ORCA-ER CCD digital camera, filter sets appropriate for Cy3 and DAPI, and Scanalytics IPLab v3.5.5 scientific imaging software. Consistent exposure times of 1 and 5 s were used for DAPI and Cy3 images, respectively. We segmented DAPI images using IPLab software and overlaid them on corresponding Cy3 image segmentations to identify positive probe signals with corresponding DAPI signals.

Negative control counts were determined using the same technique and subtracted from positive probe counts to correct for autofluorescence and nonspecific binding. We counted an average of 693 DAPI-staining cells for surface samples from 1 to 150 m (*n* = 72), and an average of 320 DAPI staining cells for mesopelagic samples from 250 to 3,000 m (*n* = 21).

Bulk nucleic acid hybridization

Unamplified small subunit ribosomal RNA was probed essentially as described²⁷. We used only two oligonucleotide probes, SAR11-441R and SAR11-542R, from the *in situ* set of probes because these two probes could detect nearly all representative SAR11 clade 16S rRNA sequences and because the additive effect on intensity needed to identify small cells using FISH was not necessary. Stringency conditions used for this study were determined empirically. Individually determined hybridization wash temperatures were 42 °C for the SAR11 probes, making it possible to combine the two SAR11 probes used in this study into a single probe set. The SAR11 signal was compared with the total bacterial RNA signal obtained using probe EUB-338Rpl and the specific hybridization value was determined by comparison with the SAR11 positive control strains, HTCC1040 and HTCC1062 (ref. 22).

Received 31 May; accepted 7 October 2002; doi:10.1038/nature01240.

- Giovannoni, S. & Rappé, M. *Microbial Ecology of the Oceans* (ed. Kirchman, D. L.) 47–84 (John Wiley and Sons, New York, 2000).
- Cho, B. C. & Azam, F. Major role of bacteria in biogeochemical fluxes in the ocean's interior. *Nature* **332**, 441–443 (1988).
- Fuhrman, J. A., Sleetor, T. D., Carlson, C. A. & Proctor, L. Dominance of bacterial biomass in the Sargasso Sea and its ecological implications. *Mar. Ecol. Prog. Ser.* **57**, 207–217 (1989).
- Buck, K. R., Chavez, F. P. & Campbell, L. Basin-wide distributions of living carbon components and the inverted trophic pyramid of the central gyre of the North Atlantic Ocean, summer 1993. *Aquat. Microb. Ecol.* **10**, 238–298 (1996).
- Carlson, C. A., Ducklow, H. W. & Sleetor, T. D. Stocks and dynamics of bacterioplankton in the northwestern Sargasso Sea. *Deep-Sea Res. II* **43**, 491–516 (1996).
- Karner, M. B., Delong, E. F. & Karl, D. M. Archaeal dominance in the mesopelagic zone of the Pacific Ocean. *Nature* **409**, 507–510 (2001).
- Fuhrman, J. A. & Ouverney, C. C. Marine microbial diversity studied via 16S rRNA sequences: cloning results from coastal waters and counting native archaea with fluorescent single cell probes. *Aquat. Ecol.* **32**, 3–15 (1998).
- Wintzingerode, F. V., Gobel, U. B. & Stackebrandt, E. Determination of microbial diversity in environmental samples: pitfalls of PCR-based rRNA analysis. *FEMS Microbiol. Rev.* **21**, 213–229 (1997).
- Hicks, R. E., Amann, R. I. & Stahl, D. A. Dual staining of natural bacterioplankton with 4' 6-diamidino-2-phenylindole and fluorescent oligonucleotide probes targeting kingdom-level 16S rRNA sequences. *Appl. Environ. Microbiol.* **58**, 2158–2163 (1992).
- DeLong, E. F., Wickham, G. S. & Pace, N. R. Phylogenetic stains: ribosomal RNA-based probes for the identification of single cells. *Science* **243**, 1360–1363 (1989).
- Amann, R. I., Krumholz, L. & Stahl, D. A. Fluorescent-oligonucleotide probing of whole cells for determinative, phylogenetic, and environmental studies in microbiology. *J. Bacteriol.* **172**, 762–770 (1990).
- Glöckner, F. O. et al. An *in situ* hybridization protocol for detection and identification of planktonic bacteria. *Syst. Appl. Microbiol.* **19**, 403–406 (1996).
- Frischer, M. E., Floriani, P. J. & Nierzwicki-Bauer, S. A. Differential sensitivity of 16S rRNA targeted oligonucleotide probes used for fluorescence *in situ* hybridization is a result of ribosomal higher order structure. *Can. J. Microbiol.* **42**, 1061–1071 (1996).
- Fuchs, B. M. et al. Flow cytometric analysis of the *in situ* accessibility of *Escherichia coli* 16S rRNA for fluorescently labeled oligonucleotide probes. *Appl. Environ. Microbiol.* **64**, 4973–4982 (1998).
- Fuchs, B. M., Glöckner, F. O., Wulf, J. & Amann, R. Unlabeled helper oligonucleotides increase the *in situ* accessibility to 16S rRNA of fluorescently labeled oligonucleotide probes. *Appl. Environ. Microbiol.* **66**, 3603–3607 (2000).
- Lee, S., Malone, C. & Kemp, P. F. Use of multiple 16S rRNA-targeted fluorescent probes to increase signal strength and measure cellular RNA from natural planktonic bacteria. *Mar. Ecol. Prog. Ser.* **101**, 193–201 (1993).
- Schonhuber, W., Fuchs, B., Juretschko, S. & Amann, R. I. Improved sensitivity of whole-cell hybridization by the combination of horseradish peroxidase-labeled oligonucleotides and tyramide signal amplification. *Appl. Environ. Microbiol.* **63**, 3268–3273 (1997).
- Pernthaler, A., Preston, C. M., Pernthaler, J., DeLong, E. F. & Amann, R. Comparison of fluorescently labeled oligonucleotide and polynucleotide probes for the detection of pelagic marine bacteria and archaea. *Appl. Environ. Microbiol.* **68**, 661–667 (2002).
- Sieracki, M. E., Johnson, P. W. & Sieburth, J. M. Detection, enumeration, and sizing of planktonic bacteria by image-analyzed epifluorescence microscopy. *Appl. Environ. Microbiol.* **49**, 799–810 (1985).
- Porter, K. G. & Feig, Y. S. The use of DAPI for identifying and counting aquatic microflora. *Limnol. Oceanogr.* **25**, 943–948 (1980).
- Kemp, P. F., Lee, S. & LaRoche, J. Estimating the growth rate of slowly growing marine bacteria from RNA content. *Appl. Environ. Microbiol.* **59**, 2594–2601 (1993).
- Rappé, M. S., Connon, S. A., Vergin, K. L. & Giovannoni, S. J. Cultivation of the ubiquitous SAR11 marine bacterioplankton clade. *Nature* **418**, 630–633 (2002).
- Cottrell, M. T. & Kirchman, D. L. Community composition of marine bacterioplankton determined by 16S rRNA gene clone libraries and fluorescence *in situ* hybridization. *Appl. Environ. Microbiol.* **66**, 5116–5122 (2000).
- Whitman, W. B., Coleman, D. C. & Wiebe, W. J. Prokaryotes: The unseen majority. *Proc. Natl Acad. Sci. USA* **95**, 6578–6583 (1998).
- Field, K. G. et al. Diversity and depth-specific distribution of SAR11 cluster rRNA genes from marine planktonic bacteria. *Appl. Environ. Microbiol.* **63**, 63–70 (1997).
- Ludwig, W. et al. Bacterial phylogeny based on comparative sequence analysis. *Electrophoresis* **19**, 554–568 (1998).
- Giovannoni, S. J., Britschgi, T. B., Moyer, C. L. & Field, K. G. Genetic diversity in Sargasso Sea bacterioplankton. *Nature* **345**, 60–63 (1990).

Acknowledgements We thank R. Parsons, N. Nelson, the BATS scientific team and officers and crew of the RV *Weatherbird II* for help with collecting and processing samples. This work was supported by grants from Oregon State University, the Murdock Charitable Trust and the National Science Foundation.

Competing interests statement The authors declare that they have no competing financial interests.

Correspondence and requests for materials should be addressed to S.J.G. (e-mail: steve.giovannoni@orst.edu).

Macroevolution simulated with autonomously replicating computer programs

Gabriel Yedid*† & Graham Bell*

* Biology Department, McGill University, 1205 avenue Dr Penfield, Montreal, Quebec, Canada H3A 1B1

† The Center for Microbial Ecology, 540 Plant and Soil Sciences Building, Michigan State University, East Lansing, Michigan 48824-1325, USA

The process of adaptation occurs on two timescales. In the short term, natural selection merely sorts the variation already present in a population, whereas in the longer term genotypes quite different from any that were initially present evolve through the cumulation of new mutations. The first process is described by the mathematical theory of population genetics. However, this theory begins by defining a fixed set of genotypes and cannot provide a satisfactory analysis of the second process because it does not permit any genuinely new type to arise. The evolutionary outcome of selection acting on novel variation arising over long periods is therefore difficult to predict. The classical problem of this kind is whether ‘replaying the tape of life’ would invariably lead to the familiar organisms of the modern biota^{1,2}. Here we study the long-term behaviour of populations of autonomously replicating computer programs and find that the same type, introduced into the same simple environment, evolves on any given occasion along a unique trajectory towards one of many well-adapted end points.

When replicate lines of microbes are cultured in the same conditions, they usually evolve higher rates of growth in parallel. In principle, this need involve no more than the successive substitution of the same series of mutations and thus the emergence of the same multilocus genotype^{2,3}. The tempo of adaptation can be analysed through the theory of periodic selection^{4,5}; the lack of substantial genetic variance of fitness among replicate lines suggests that this simple description might often be adequate^{6,7}. In a few cases where the relevant loci are known this has been confirmed directly^{8–10}, but in other experiments replicate lines have diverged in fitness¹¹, or the pattern of correlated responses has shown that they have diverged genetically, despite their similar direct responses^{12,13}. In some cases, the physiological and genetic responses occurring in replicate lines have been identified, showing how the same selection pressure can lead to quantitatively and qualitatively different outcomes^{14,15}. In experiments with large multicellular organisms such as *Drosophila*, differences among replicate lines can be caused by initial differences among the founding populations, or by inbreeding or drift during the course of the experiment^{16,17}. In microbial experiments with large populations of asexual organisms derived from isogenic founders, these explanations are ruled out, raising the possibility that long-term evolutionary change is often highly contingent.

We studied an auto-adaptive genetic system called Tierra^{18,19}, comprising a virtual microcosm inhabited by self-replicating computer programs (‘creatures’). The genome of each creature is a sequence of instructions that directs the flow of control. Each instruction performs some elementary operation, such as incrementing a register or moving the instruction pointer to another location in the genome. When an appropriate sequence of instructions is correctly executed, the sequence is copied elsewhere in computer memory; changing the sequence of instructions usually changes the rate of replication. Selection between the variants produced by mutation is caused by competition for CPU time: variants that replicate more rapidly tend to increase in frequency. The evolving population of programs thus resembles an evolving population of bacteria or viruses, and such auto-adaptive genetic systems are now coming into use to supplement conventional analytical methods in evolutionary theory²⁰. We have shown previously that the microevolutionary dynamics of Tierran populations are adequately described by conventional population genetics theory²¹.

We began each experiment with a single creature that was allowed to proliferate indefinitely, with an initial carrying capacity of 500 individuals and a mutation rate of 0.1 per genome per replication.

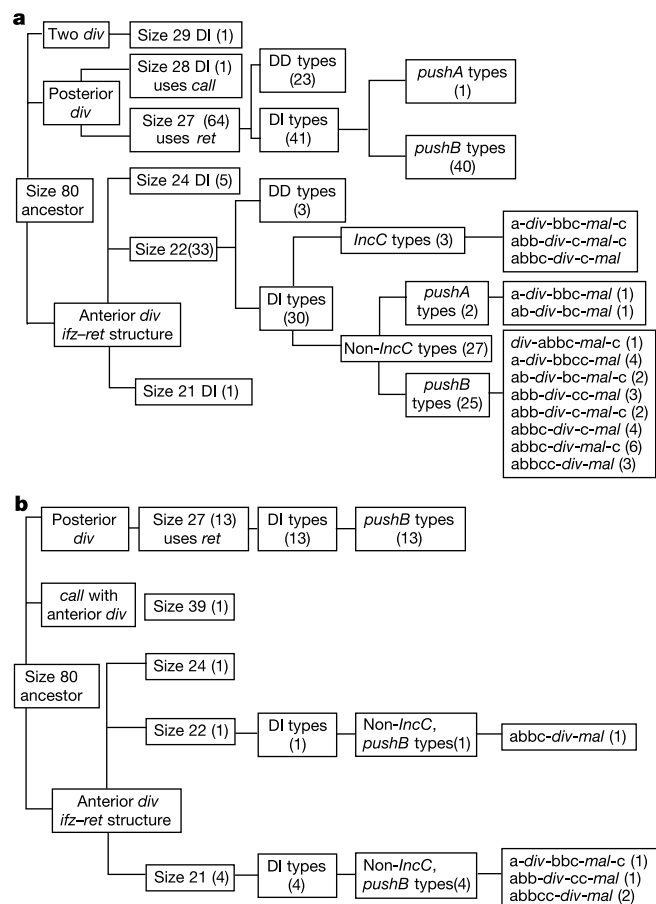


Figure 1 Variety of evolutionary end points. Genotypes are classified according to the presence and position of key instructions such as *div* (divide), *mal* (allocate memory), *IncC* (increment register C), *PushX* (put a value in register X onto a stack), *ifz* (if register equals zero then execute next instruction, else advance two instructions) and *ret* (return). DD types are density-dependent and cannot replicate as single copies in pure culture; DI types are density-independent. The diversity of size-22 DI types is arranged according to the position of instructions relative to *div* and *mal*: a is *adrb* or *adra*; b is *subAAC* or *movBA*; c is *subCAB* or *pushB*. The numbers in parentheses give the number of observed outcomes of a given kind. **a**, Small-population experiments; **b**, large-population experiments.